European Journal of Medicinal Chemistry 64 (2013) 90–98

Contents lists available at SciVerse ScienceDirect

European Journal of Medicinal Chemistry

journal homepage: http://www.elsevier.com/locate/ejmech

Original article

^{99m}Tc-labeled dibenzylideneacetone derivatives as potential SPECT probes for *in vivo* imaging of β-amyloid plaque

Yanping Yang, Mengchao Cui*, Bing Jin, Xuedan Wang, Zijing Li, Pingrong Yu, Jianhua Jia, Hualong Fu, Hongmei Jia, Boli Liu*

Key Laboratory of Radiopharmaceuticals, Ministry of Education, College of Chemistry, Beijing Normal University, Beijing 100875, PR China

ARTICLE INFO

Article history:
Received 22 February 2013
Received in revised form
25 March 2013
Accepted 27 March 2013
Available online 6 April 2013

Keywords:
Alzheimer's disease
β-Amyloid plaque
Dibenzylideneacetone
Technetium-99m
SPECT imaging

ABSTRACT

Four ^{99m}Tc-labeled dibenzylideneacetone derivatives and corresponding rhenium complexes were successfully synthesized and biologically evaluated as potential imaging probes for Aβ plaques using SPECT. All rhenium complexes (**5a**–**d**) showed affinity for $A\beta_{(1-42)}$ aggregates (K_i = 13.6–120.9 nM), and selectively stained the Aβ plaques on brain sections of transgenic mice. Biodistribution in normal mice revealed that [^{99m}Tc]**5a**–**d** exhibited moderate initial uptake (0.31%–0.49% ID/g at 2 min) and reasonable brain washout at 60 min post-injection. Although additional optimizations are still needed to facilitate it's penetration through BBB, the present results indicate that [^{99m}Tc]**5a** may be a potential SPECT probe for imaging Aβ plaques in Alzheimer's brains.

1. Introduction

Alzheimer's disease (AD) is a neurodegenerative disorder characterized by the devastating loss of memory and cognitive abilities, and it will afflict about 63 million people by 2030, and 114 million by 2050 worldwide [1–3]. The deposition of extracellular β-amyloid (Aβ) plaques and intracellular neurofibrillary tangles (NFTs) containing highly phosphorylated tau protein in the brain have been regarded as the dominant factors driving AD pathogenesis [4]. Currently, the diagnosis of AD primarily depends on clinical evaluation, patient history, structural and functional imaging of the brain by computed tomography (CT) and magnetic resonance imaging (MRI) [5,6]. However, these methods are usually insufficient and unreliable in the definite diagnosis of AD, especially for patients in early stage [7]. The final diagnosis of AD can be accomplished only by postmortem examination of brain tissues. As the accumulation of Aβ plaques and NFTs in AD brains occurs 20–40 years before the onset of clinical symptoms [8], detecting their changes *in vivo* may impressively facilitate early diagnosis and monitoring the progression of AD. Therefore, there is an urgent need for *in vivo* imaging of Aβ plaques with the assistance of noninvasive techniques such as positron emission tomography (PET) or single photon emission computed tomography (SPECT).

Over recent years, a big variety of PET probes based on Congo Red (CR) and Thioflavin-T (ThT) have been synthesized and evaluated for imaging Aβ plaques. Among them, [^{11}C]-4-*N*-methylamino-4′-hydroxystilbene ([^{11}C]SB-13) [9,10], [^{11}C]-2-(4-(methylamino) phenyl)-6-hydroxybenzothiazol ([^{11}C]PIB) [11,12], [^{18}F]-4-(*N*-methylamino)-4′-(2-(2-(2-fluoroethoxy)ethoxy)ethoxy)-stilbene ([^{18}F] BAY94-9172) [13–15], [^{18}F]-2-(3-fluoro-4-methyaminophenyl)benzothiazol-6-ol ([^{18}F]GE-067) [16] and [^{18}F]-(*E*)-4-(2-(6-(2-(2-(2-fluoroethoxy)ethoxy)ethoxy)pyridin-3-yl)vinyl)-*N*-methylaniline ([^{18}F]AV-45) [17–19] have been evaluated clinically and demonstrated potential utilization. The imaging of Aβ plaques *in vivo* with PET has achieved remarkable progress so far, while the development of SPECT tracers lags far behind. When compared with PET, SPECT have several certain advantages including lower cost, widespread availability, and the use of isotopes with longer half-lives. Hence extraordinary efforts should be spent on the innovation of SPECT probes for Aβ imaging.

Among the radioisotopes used in diagnostic imaging nuclear medicine by SPECT, ^{99m}Tc ($T_{1/2}$ = 6.01 h, γ (89%): 141 keV) is the most widely used and can even be regarded as a star radioisotope due to the following aspects: it is readily produced by a commercial ^{99}Mo/^{99m}Tc generator, besides, it's moderate gamma-ray energy and physical half-life extremely fulfill the SPECT imaging requirements

* Corresponding authors. Tel./fax: +86 10 58808891.
E-mail addresses: cmc@bnu.edu.cn (M. Cui), liuboli@bnu.edu.cn (B. Liu).

0223-5234/$ – see front matter © 2013 Elsevier Masson SAS. All rights reserved.
http://dx.doi.org/10.1016/j.ejmech.2013.03.057

by providing good biological localization and appropriate residence time. Thus, new ^{99m}Tc-labeled Aβ imaging probes will provide simple, convenient, economical and widespread SPECT-based imaging methods for the early diagnosis of AD. In the past decade, a great deal of research has been conducted in this field. Initially reported ^{99m}Tc-labeled CR [20,21] and Chrysamine G derivatives [22,23], which displayed high affinity for Aβ aggregates *in vitro*, failed to cross the blood–brain barrier (BBB) for their high molecular weight and charged character. Then further attempts were focused on smaller, neutral, and more lipophilic ^{99m}Tc-labeled ligands. Derivatives of biphenyl [24], benzothiazole aniline [25–27], chalcone [28], flavone, aurone [29], curcumin [30], benzofuran [31,32] and benzoxazole [33] conjugated with monoamine–monoamide dithiol (MAMA) and bis(aminoethanethiol) (BAT) chelating ligands (Fig. 1) have been synthesized and evaluated as potential Aβ imaging probes, unfortunately, none of them showed specific binding to Aβ plaques *in vivo* due to either low affinity or low uptake in the brain.

Recently, based on the structure of curcumin, an extensive series of dibenzylideneacetone derivatives developed as a novel molecular scaffold for Aβ imaging were reported [34]. Structure–activity relationships revealed that the *para* position on the phenyl ring of dibenzylideneacetone showed extraordinarily high tolerance for steric bulk substitutions. Increasing the size of the substituent has negligible impact on the affinity for Aβ aggregates, and even when the ligand was substituted by a bulky trityloxy group also exhibited high affinity ($K_i = 2.8 \pm 0.4$ nM). This encouraging finding inspires us that the introduction of a large ^{99m}Tc chelating structure probably won't bring about a considerable change in the binding properties.

In the present study, we designed four novel ^{99m}Tc-labeled dibenzylideneacetone derivatives (Fig. 2) conjugated to MAMA and BAT via a propoxy or pentyloxy spacer for Aβ plaque imaging. Hereon, we report the synthesis and preliminary biological evaluation of these novel ^{99m}Tc-labeled dibenzylideneacetone derivatives as potential SPECT probes for imaging Aβ plaques in AD.

2. Results and discussion

2.1. Chemistry

The synthesis of ^{99m}Tc/Re dibenzylideneacetone derivatives is outlined in Scheme 1. The key step in the formation of the dibenzylideneacetone skeleton was accomplished by base catalyzed Claisen condensation reaction starting from (*E*)-4-(4-(dimethylamino)phenyl)but-3-en-2-one and substituted benzaldehyde (**2a** or **2b**). Claisen condensation afforded compound **3a** and **3b** in yields of 54.6% and 48.9%, respectively. Then, a BAT or MAMA chelating group was conjugated with bromo-aliphatic compounds **3a** or **3b** by reacting them with Tr-Boc-BAT or Tr-MAMA, which achieved **4a**–**d** in yields of 36.0%, 27.1%, 50.8% and 54.1%, respectively. The structural and biochemical properties of ^{99m}Tc correlate well with those of Re, thus Re complexes have been usually adopted as surrogates for ^{99m}Tc complexes for structure identifications and biological evaluations [35,36]. After deprotection of the thiol groups in **4a**–**d** by trifluoroacetic acid (TFA) and triethylsilane, the rhenium complexes **5a**–**d** were prepared through a reaction with $(PPh_3)_2ReOCl_3$ in CH_2Cl_2 in 15.5–37.0% yields.

2.2. In vitro binding studies using A$\beta_{(1–42)}$ aggregates

The binding affinities of rhenium complexes **5a**–**d** for A$\beta_{(1–42)}$ aggregates were evaluated by competition binding assay using [^{125}I]6-iodo-2-(4′-dimethylamino)-phenyl-imidazo[1,2-a]pyridine, [^{125}I]IMPY, as the competing radio-ligand according to conventional methods [34]. IMPY was also tested using the same system for comparison. As shown in Table 1, compounds with the MAMA cheating ligand, **5c** and **5d**, exhibited moderate binding affinity to A$\beta_{(1–42)}$ aggregates (K_i = 120.9 and 59.1 nM, respectively), while compounds with the BAT cheating ligand, **5a** and **5b**, displayed high affinity (K_i = 24.7 and 13.6 nM, respectively) which was comparable to the value of IMPY ($K_i = 11.5$ nM), indicating that they hold sufficient affinity for A$\beta_{(1–42)}$ aggregates *in vitro*. This result

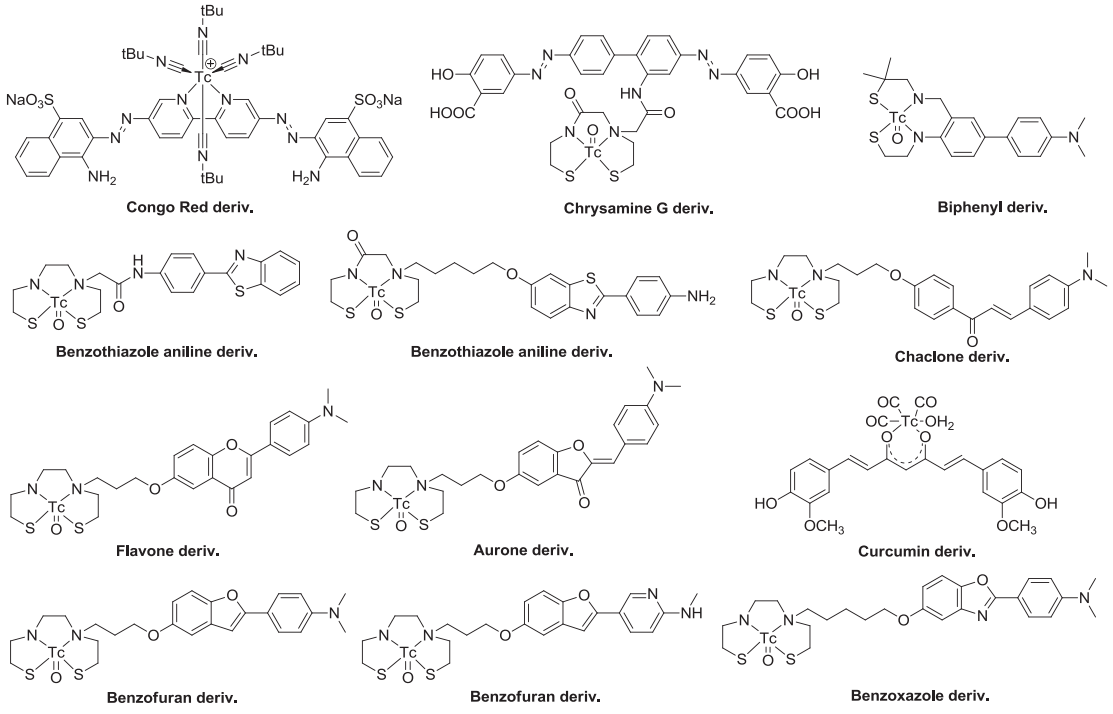

Fig. 1. Chemical structure of ^{99m}Tc-labeled Aβ imaging probes reported previously.

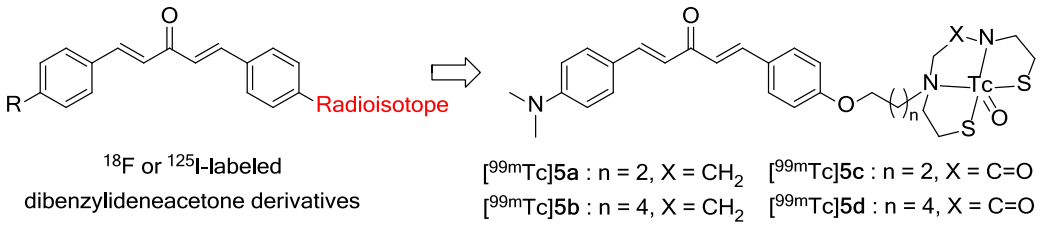

Fig. 2. Chemical structure of ^{99m}Tc-labeled dibenzylideneacetone derivatives reported in the present study.

demonstrates that the introduction of the bulky BAT chelating group didn't interfere with the binding to A$\beta_{(1-42)}$ aggregates observably. When considering the impact on affinity bring by the length of spacers, the result indicated that the affinity of compounds **5b** and **5d**, with longer pentyloxy spacer, was considerably higher than that of compounds with propoxy spacer. As expected, when the spacer getting longer, the interference of the large ^{99m}Tc chelating structure on the binding property of targeting molecule (dibenzylideneacetone) is smaller, and thus the affinity was maintained preferably.

2.3. *In vitro* fluorescent staining

In vitro fluorescent staining of Aβ plaques on sections of brain tissue from a transgenic (Tg) model mice (C57BL6, APPswe/PSEN1, 11 months old) and an age-matched control mice were conducted to confirm the specific and high binding affinity of compounds **5a**–**d** to Aβ plaques (Fig. 3). Fluorescent staining images revealed that these four rhenium complexes all displayed excellent labeling of Aβ plaques on the sections of Tg mice with low background (Fig. 3A, D, G and J), while there was no notable staining in the age-matched control mice (Fig. 3C, F, I and L). The distribution of Aβ plaques was consistent with the results of fluorescent staining with Thioflavin-S on the adjacent sections (Fig. 3B, E, H and K). The results incontestably manifested that these rhenium complexes could bind specifically to Aβ plaques with low background.

2.4. Radiolabeling

The novel radio-labeled ligands [^{99m}Tc]**5a**–**d** were prepared by a ligand exchange reaction employing the precursor **4a**–**d** and ^{99m}Tc-glucoheptonate (^{99m}Tc-GH) in boiling water with radiochemical yields of 31.8%, 43.8%, 47.9% and 37.7%, respectively. After purification by high-performance liquid chromatography (HPLC), the radiochemical purity of these radiotracers was higher than 95%. The radiochemical identities of the ^{99m}Tc-labeled tracers were affirmed by comparison of the retention times on HPLC column with that of the corresponding Re complexes (Table 2, see Supporting information). The retention times of [^{99m}Tc]**5a**–**d** on HPLC column were 10.45, 10.88, 15.18 and 15.36 min, and that of the corresponding rhenium complexes **5a**–**d** were 8.97, 9.29 13.26 and 13.43 min, respectively. The approximation of retention times between ^{99m}Tc-labeled tracers and corresponding rhenium complexes sufficiently suggested that the desired ^{99m}Tc-labeled dibenzylideneacetone derivatives were successfully generated.

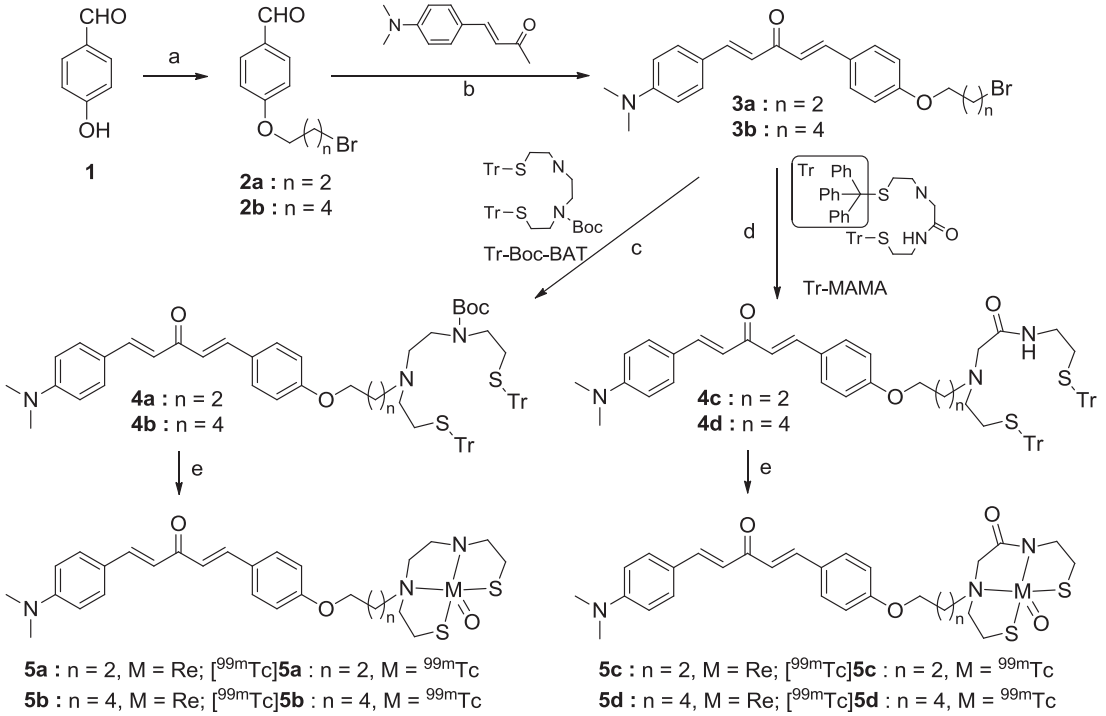

Scheme 1. Reagents and conditions: (a) 1,3-dibromopropane (or 1,5-dibromopentane), K_2CO_3, MeCN, 90 °C; (b) $NaOCH_3$, CH_3CH_2OH, r.t.; (c) Tr-Boc-BAT, K_2CO_3, MeCN, 90 °C; (d) Tr-MAMA, K_2CO_3, MeCN, 90 °C; (e) (1) TFA, Et_3SiH; (2) ^{99m}Tc-GH, 100 °C; or $(PPh_3)ReOCl_3$, CH_2Cl_2, CH_3OH, 90 °C.

Table 1
Inhibition constants for the binding of [^{125}I]IMPY to A$\beta_{(1-42)}$ aggregates.

Compound	K_i (nM)[a]
5a	24.7 ± 6.1
5b	13.6 ± 7.8
5c	120.9 ± 4.3
5d	59.1 ± 24.0
IMPY	11.5 ± 2.5

[a] Measured in triplicate with values given as the mean ± SD.

2.5. Partition coefficient determination

The log *D* values of [^{99m}Tc]**5a**–**d** were 3.42 ± 0.02, 3.17 ± 0.04, 3.53 ± 0.01, and 3.57 ± 0.17, respectively (Table 2), which are all in an optimal range (1–3.5) for BBB penetration, indicating that the four tracers have appropriate lipophilicity suitable for brain imaging.

Table 2
HPLC retention times of ^{99m}Tc-labeled dibenzylideneacetone derivatives and corresponding Re complexes and log *D* values of [^{99m}Tc]**5a**–**d**.

^{99m}Tc compound	Retention time (min)	Re compound	Retention time (min)	Log *D* of ^{99m}Tc compound[c]
[^{99m}Tc]**5a**[a]	10.45	**5a**	8.97	3.36 ± 0.08
[^{99m}Tc]**5b**[a]	10.88	**5b**	9.29	3.17 ± 0.10
[^{99m}Tc]**5c**[b]	15.18	**5c**	13.26	3.52 ± 0.10
[^{99m}Tc]**5d**[b]	15.36	**5d**	13.43	3.57 ± 0.15

[a] Reversed-phase HPLC using a binary gradient system (acetonitrile/water:80%/20%) at a 1.0 mL/min flow rate.
[b] Reversed-phase HPLC using a binary gradient system (acetonitrile/water:70%/30%) at a 1.0 mL/min flow rate.
[c] Measured in triplicate with values expressed as the mean ± SD.

2.6. In vivo biodistribution in normal mice

Biodistribution experiments in normal ICR mice (5 weeks, male) were carried out to evaluate the pharmacokinetics of ^{99m}Tc-labeled dibenzylideneacetone tracers *in vivo* (Table 3). A biodistribution

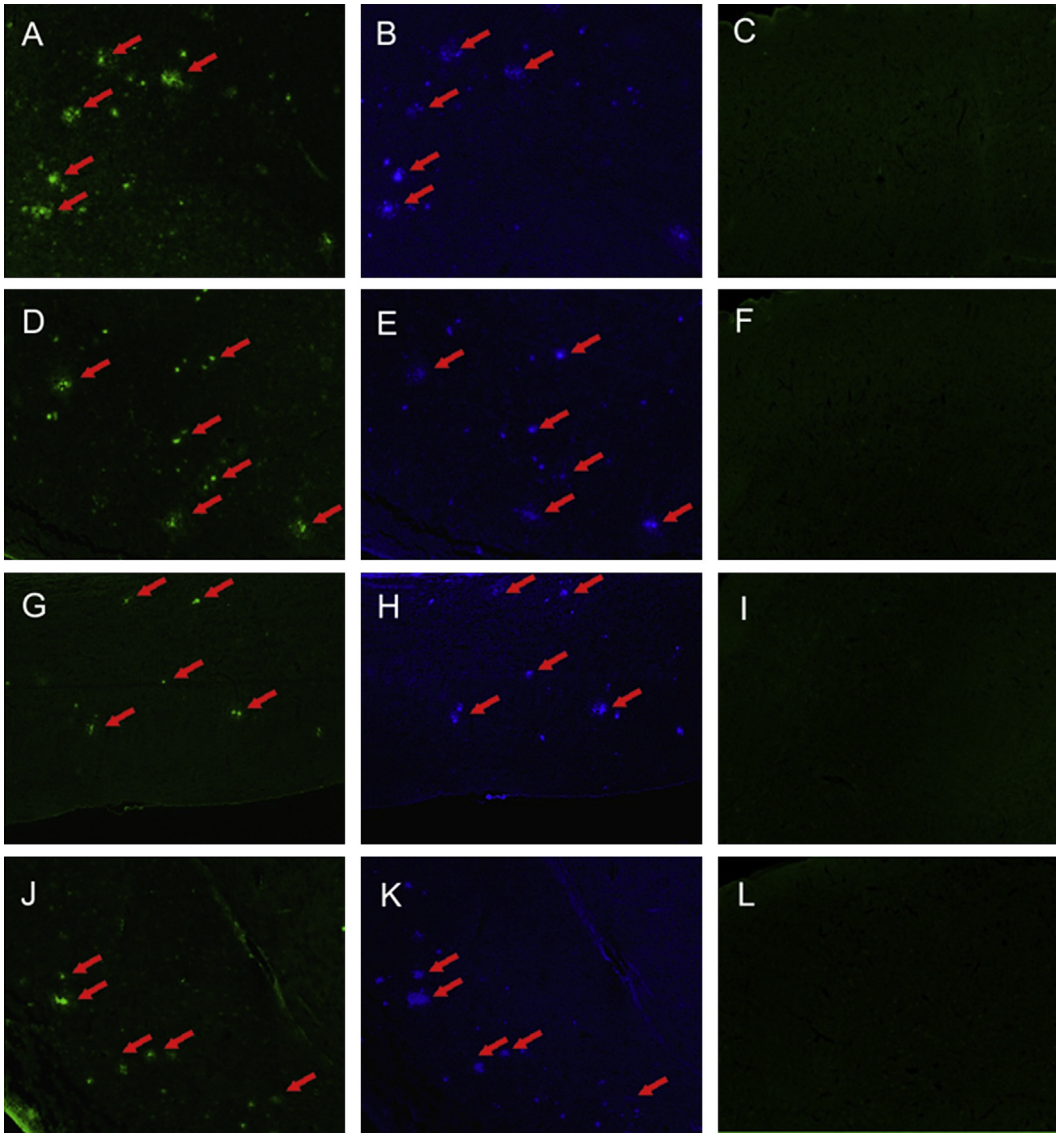

Fig. 3. *In vitro* fluorescent staining of Aβ plaques by compounds **5a**–**d** on brain sections of a Tg model mouse (C57BL6, APPswe/PSEN1, 11 months old, male) with a DAPI filter (A, D, G and J). The presence and distribution of Aβ plaques on the adjacent sections were confirmed with Thioflavin-S with an AF filter (B, E, H and K). Fluorescence staining of compounds **5a**–**d** on brain sections of a normal mouse was also carried out as control (C, F, I and L).

Table 3
Biodistribution of radioactivity after injection of [^{99m}Tc]**5a**–**d** in normal ICR mice.[a]

Organ	2 min	10 min	30 min	60 min
[^{99m}Tc]**5a** (log D = 3.36 ± 0.08)				
Blood	6.36 ± 1.19	1.61 ± 0.18	0.71 ± 0.09	0.61 ± 0.07
Brain	0.49 ± 0.08	0.23 ± 0.04	0.12 ± 0.03	0.08 ± 0.01
Heart	10.23 ± 1.20	2.43 ± 0.20	0.86 ± 0.15	0.53 ± 0.06
Liver	26.69 ± 4.08	26.22 ± 0.91	17.57 ± 1.42	12.58 ± 3.90
Spleen	3.03 ± 0.61	1.67 ± 0.37	0.95 ± 0.23	0.55 ± 0.14
Lung	17.66 ± 3.05	6.05 ± 1.82	1.44 ± 0.56	0.89 ± 0.14
Kidney	21.45 ± 2.66	13.2 ± 2.81	6.96 ± 1.76	5.97 ± 1.16
Pancreas	3.78 ± 0.66	2.74 ± 0.61	1.09 ± 0.37	0.52 ± 0.11
Stomach[b]	1.10 ± 0.18	1.64 ± 0.54	2.55 ± 0.78	1.53 ± 0.13
Intestine[b]	5.77 ± 0.72	12.02 ± 1.41	25.04 ± 4.70	54.01 ± 6.54
[^{99m}Tc]**5b** (log D = 3.17 ± 0.10)				
Blood	7.21 ± 1.38	1.25 ± 0.08	0.80 ± 0.05	0.52 ± 0.05
Brain	0.47 ± 0.11	0.27 ± 0.03	0.19 ± 0.03	0.12 ± 0.02
Heart	29.79 ± 5.78	11.72 ± 1.75	10.12 ± 3.29	6.63 ± 1.32
Liver	77.67 ± 18.54	56.22 ± 9.89	52.99 ± 4.78	43.84 ± 6.36
Spleen	16.64 ± 2.62	9.08 ± 1.25	5.68 ± 1.53	4.06 ± 0.71
Lung	11.87 ± 2.56	3.84 ± 1.09	2.42 ± 0.57	1.75 ± 0.16
Kidney	12.33 ± 3.20	7.93 ± 1.24	5.02 ± 0.27	3.41 ± 0.48
Pancreas	4.21 ± 0.76	4.80 ± 0.82	2.74 ± 0.87	1.44 ± 0.21
Stomach[b]	1.56 ± 0.75	3.72 ± 0.79	5.09 ± 2.15	1.57 ± 0.60
Intestine[b]	5.97 ± 1.22	25.67 ± 6.08	54.31 ± 6.14	60.14 ± 16.90
[^{99m}Tc]**5c** (log D = 3.52 ± 0.10)				
Blood	4.87 ± 0.76	1.30 ± 0.12	0.60 ± 0.05	0.42 ± 0.02
Brain	0.48 ± 0.06	0.19 ± 0.02	0.10 ± 0.02	0.09 ± 0.01
Heart	14.24 ± 1.21	3.89 ± 0.18	1.33 ± 0.28	0.90 ± 0.12
Liver	23.67 ± 2.24	21.38 ± 3.39	18.86 ± 0.71	16.61 ± 3.98
Spleen	4.40 ± 0.30	2.19 ± 0.26	0.94 ± 0.09	0.52 ± 0.11
Lung	24.52 ± 3.50	9.24 ± 2.20	3.06 ± 0.43	1.15 ± 0.31
Kidney	16.51 ± 0.66	9.03 ± 1.66	4.91 ± 0.76	3.86 ± 0.46
Pancreas	4.28 ± 0.30	3.46 ± 0.52	2.11 ± 0.34	1.24 ± 0.30
Stomach[b]	1.14 ± 0.09	1.40 ± 0.12	1.12 ± 0.05	1.68 ± 0.51
Intestine[b]	5.73 ± 0.62	12.09 ± 0.70	30.47 ± 6.84	39.15 ± 7.12
[^{99m}Tc]**5d** (log D = 3.57 ± 0.15)				
Blood	5.10 ± 0.37	2.32 ± 0.54	1.29 ± 0.15	1.21 ± 0.24
Brain	0.31 ± 0.06	0.22 ± 0.02	0.11 ± 0.04	0.15 ± 0.02
Heart	14.56 ± 0.67	4.17 ± 0.33	1.75 ± 0.41	1.14 ± 0.19
Liver	42.12 ± 9.68	43.73 ± 4.71	29.40 ± 4.31	25.97 ± 5.95
Spleen	5.97 ± 1.76	2.63 ± 0.24	1.67 ± 0.70	1.35 ± 0.49
Lung	12.03 ± 2.92	4.20 ± 0.49	1.64 ± 0.28	1.24 ± 0.22
Kidney	16.85 ± 1.16	12.07 ± 2.72	6.45 ± 1.41	4.85 ± 0.94
Pancreas	4.90 ± 0.69	5.50 ± 1.25	3.44 ± 0.91	1.93 ± 0.47
Stomach[b]	1.34 ± 0.13	2.05 ± 0.39	2.82 ± 0.72	6.42 ± 1.10
Intestine[b]	5.20 ± 0.58	21.46 ± 2.27	35.03 ± 5.70	54.66 ± 11.20

[a] Expressed as % injected dose per gram. Each value represents the mean ± SD for 4–5 mice.
[b] Expressed as % injected dose per organ.

study provides crucial information on penetration of the BBB and radioactivity pharmacokinetics *in vivo*. [^{99m}Tc]**5a**–**d** all showed the highest initial uptake at 2 min post-injection, 0.49, 0.47, 0.48 and 0.31% ID/g, respectively. Although the values were comparable or slightly lower than that of ^{99m}Tc-labeled tracers reported previously (0.2–1.80% ID/g) [24–26,28–32], [^{99m}Tc]**5a** and [^{99m}Tc]**5b** can also expect excellent labeling of Aβ plaques *in vivo* due to their high affinities. The brain$_{2min}$/brain$_{60min}$ ratio of [^{99m}Tc]**5a**–**c** were 6.13, 3.92 and 5.33, respectively, which were superior than that of ^{99m}Tc-labeled phenylbenzothiazole (2.06) [26], phenylbenzofuran (2.39) [31], pyridylbenzofuran (2.28) [32], phenylbenzoxazole (3.24) [33] and so on. This data undoubtedly indicated that all the four tracers possessed good clearance property from the normal brain. The accumulation of radioactivity was observed predominantly in liver and kidney at the early stage, and then dropped gradually with time, while continuous gastrointestinal accumulation of the radiotracers resulted in a high intestine uptake at later time periods.

3. Conclusion

In conclusion, four ^{99m}Tc-labeled dibenzylideneacetone derivatives and their corresponding rhenium complexes were successfully synthesized and biologically evaluated as SPECT imaging probes for Aβ plaques. *In vitro* binding studies indicated that rhenium complexes **5a**–**d** displayed moderate to high affinity for A$\beta_{(1-42)}$ aggregates varied from 13.6 to 120.9 nM. The high binding affinity was further confirmed by fluorescent staining, and all the dibenzylideneacetone derivatives specifically labeled Aβ plaques on the brain sections of Tg mice. Biodistribution in normal mice revealed that [^{99m}Tc]**5a** exhibited moderate initial uptake (0.49% ID/g at 2 min) and fast washout from the brain, with a brain$_{2min}$/brain$_{60min}$ ratio of 6.13. All in all, the preliminary results suggest that the [^{99m}Tc]**5a** may be a potential SPECT probe for imaging Aβ plaques in Alzheimer's brains. But additional chemical refinements are earnestly required to further improve the penetration through BBB.

4. Experimental

4.1. General information

All reagents used for chemical synthesis were commercial products and were used without further purification. Na^{99m}TcO$_4$ was obtained from a commercial ^{99}Mo/^{99m}Tc generator, Beijing Atomic High-tech Co. All ^{1}H NMR spectra were acquired at 400 MHz on Bruker Avance III NMR spectrometers in $CDCl_3$ solutions at room temperature with trimethylsilyl (TMS) as an internal standard. Chemical shifts were reported as δ values relative to the internal TMS, and Coupling constants were reported in hertz. The multiplicity is defined by s (singlet), d (doublet), t (triplet), and m (multiplet). Mass spectra were acquired with a micrOTOF-Q II instrument. Reactions were monitored by TLC (Silica gel 60 F_{254} aluminum sheets, Merck) and compounds were visualized by illumination with a short wavelength Ultra-Violet lamp (λ = 254 nm or 365 nm). Column chromatography purification were performed on silica gel (54–74 μm) from Qingdao Haiyang Chemical Co., Ltd. HPLC was performed on a Shimadzu SCL-20 AVP (which is equipped with a Bioscan Flow Count 3200 NaI/PMT γ-radiation scintillation detector and a SPD-20A UV detector, λ = 254 nm) and a Venusil MP C18 reverse phase column (Agela Technologies, 5 μm, ID = 4.6 mm, length = 250 mm) eluted with a binary gradient system at 1.0 mL/min flow rate. Mobile phase A was water, while mobile phase B was acetonitrile. Fluorescent observation was performed by the Axio Observer Z1 inverted fluorescence microscope (Zeiss, Germany) equipped with a DAPI filter set (excitation, 405 nm) and AF488 filter set (excitation, 495 nm). Normal ICR mice (five weeks, male) were used for biodistribution experiments. Transgenic mice (C57BL6, APPswe/PSEN1, male, 11 months old), used as an Alzheimer's model, were purchased from the Institute of Laboratory Animal Science, Chinese Academy of Medical Sciences. All protocols requiring the use of mice were approved by the animal care committee of Beijing Normal University. The purity of all key compounds was proven to be more than 95% by HPLC.

4.2. 4-(3-Bromopropoxy)benzaldehyde (**2a**)

To a solution of **1** (3.67 g, 30 mmol) in CH_3CN (50 mL) was added 1,3-dibromopropane (9.10 g, 45 mmol) and K_2CO_3 (8.29 g, 60 mmol). The mixture was stirred at 90 °C for 12 h, after cooling to room temperature, solvent was removed by vacuum, and the residue was extracted with $CHCl_3$. The organic layer was dried over $MgSO_4$ and solvent was removed. The crude product was purified by silica gel chromatography (petroleum ether/AcOEt = 8/1, v/v) to give **2a** (4.41 g, 60.4%) as a colorless oil. ^{1}H NMR (400 MHz, $CDCl_3$) δ 9.89 (s, 1H, CHO), 7.84 (d, J = 8.7 Hz, 2H, ArH), 7.01 (d, J = 8.7 Hz, 2H, ArH), 4.20 (t, J = 5.8 Hz, 2H, CH_2), 3.61 (t, J = 6.3 Hz, 2H, CH_2),

2.39–2.33 (m, 2H, CH_2). HRMS (ESI): *m/z* calcd for $C_{10}H_{12}BrO_2$ 245.0000; found 245.0091 $[M + H]^+$.

4.3. 4-(5-Bromopentyloxy)benzaldehyde (**2b**)

The procedure described above for the preparation of **2a** was employed to give **2b** (6.61 g, 81.2%) as a colorless oil. ^1H NMR (400 MHz, $CDCl_3$) δ 9.88 (s, 1H, CHO), 7.83 (d, $J = 8.8$ Hz, 2H, ArH), 6.99 (d, $J = 8.7$ Hz, 2H, ArH), 4.06 (t, $J = 6.3$ Hz, 2H, CH_2), 3.45 (t, $J = 6.7$ Hz, 2H, CH_2), 2.00–1.91 (m, 2H, CH_2), 1.90–1.82 (m, 2H, CH_2), 1.70–1.60 (m, 2H, CH_2). HRMS (ESI): *m/z* calcd for $C_{12}H_{16}BrO_2$ 271.0334; found 271.0438 $[M + H]^+$.

4.4. (1E,4E)-1-(4-(3-Bromopropoxy)phenyl)-5-(4-(dimethylamino) phenyl)penta-1,4-dien-3-one (**3a**)

A mixture of **2a** (3.02 g, 12.4 mmol), (*E*)-4-(4-(dimethylamino) phenyl)but-3-en-2-one (2.35 g, 12.4 mmol) and sodium methoxide (0.95 g, 25.0 mmol) in ethanol (50 mL) was stirred at room temperature overnight. The precipitate was collected by filtration and then recrystallized from ethanol to give **3a** (2.81 g, 54.6%) as a yellow solid. ^1H NMR (400 MHz, $CDCl_3$) δ 7.70 (d, $J = 15.7$ Hz, 1H, *trans* –CH=CH–), 7.67 (d, $J = 15.8$ Hz, 1H, *trans* –CH=CH–), 7.56 (d, $J = 8.7$ Hz, 2H, ArH), 7.52 (d, $J = 8.8$ Hz, 2H, ArH), 6.97 (d, $J = 15.8$ Hz, 1H, *trans* –CH=CH–), 6.93 (d, $J = 8.7$ Hz, 2H, ArH), 6.87 (d, $J = 15.7$ Hz, 1H, *trans* –CH=CH–), 6.69 (d, $J = 8.8$ Hz, 2H, ArH), 4.15 (t, $J = 5.8$ Hz, 2H, CH_2), 3.61 (t, $J = 6.4$ Hz, 2H, CH_2), 3.04 (s, 6H, $N(CH_3)_2$), 2.37–2.31 (m, $J = 6.1$ Hz, 2H, CH_2). HRMS (ESI): *m/z* calcd for $C_{22}H_{25}BrNO_2$ 414.1069; found 414.0955 $[M + H]^+$.

4.5. (1E,4E)-1-(4-(5-Bromopentyloxy)phenyl)-5-(4-(dimethylamino) phenyl)penta-1,4-dien-3-one (**3b**)

The procedure described above for the preparation of **3a** was employed to give **3b** (2.22 g, 48.9%) as a yellow solid. ^1H NMR (400 MHz, $CDCl_3$) δ 7.70 (d, $J = 15.7$ Hz, 1H, *trans* –CH=CH–), 7.67 (d, $J = 15.8$ Hz, 1H, *trans* –CH=CH–), 7.55 (d, $J = 8.7$ Hz, 2H, ArH), 7.51 (d, $J = 8.8$ Hz, 2H, ArH), 6.96 (d, $J = 15.8$ Hz, 1H, *trans* –CH=CH–), 6.90 (d, $J = 8.7$ Hz, 2H, ArH), 6.87 (d, $J = 15.8$ Hz, 1H, *trans* –CH=CH–), 6.69 (d, $J = 8.8$ Hz, 2H, ArH), 4.01 (t, $J = 6.3$ Hz, 2H, CH_2), 3.44 (t, $J = 6.7$ Hz, 2H, CH_2), 3.04 (s, 6H, $N(CH_3)_2$), 1.99–1.90 (m, 2H, CH_2), 1.88–1.79 (m, 2H, CH_2), 1.64 (m, 2H, CH_2). HRMS (ESI): *m/z* calcd for $C_{24}H_{29}BrNO_2$ 444.1361; found 444.1333 $[M + H]^+$.

4.6. tert-Butyl 2-((3-(4-((1E,4E)-5-(4-(dimethylamino)phenyl)-3-oxo penta-1,4-dienyl)phenoxy)propyl)(2-(tritylthio)ethyl)amino)ethyl(2-(tritylthio)ethyl)carbamate (**4a**)

A mixture of **3a** (294.2 mg, 0.71 mmol), tert-butyl 2-(tritylthio) ethyl(2-(2-(tritylthio)ethylamino)ethyl)carbamate (539.2 mg, 0.71 mmol) and K_2CO_3 (193.6 mg, 1.42 mmol) in acetonitrile (50 mL) was stirred at 90 °C for 48 h. The solvent was removed by vacuum, and water was added. The mixture was extracted with $CHCl_3$. The organic layers were combined and dried over anhydrous Mg_2SO_4 and evaporated dry. The crude product was purified by silica gel chromatography (petroleum ether/AcOEt = 3/1, v/v) to give **4a** (272.5 mg, 36.0% yield) as yellow solid foams. ^1H NMR (400 MHz, $CDCl_3$) δ 7.70 (d, $J = 15.6$ Hz, 1H, *trans* –CH=CH–), 7.66 (d, $J = 15.6$ Hz, 1H, *trans* –CH=CH–), 7.52 (d, $J = 8.8$ Hz, 2H, ArH), 7.48 (d, $J = 8.6$ Hz, 2H, ArH), 7.42–7.36 (m, 13H, ArH), 7.24–7.17 (m, 17H, ArH), 6.95 (d, $J = 15.8$ Hz, 1H, *trans* –CH=CH–), 6.87 (d, $J = 15.6$ Hz, 1H, *trans* –CH=CH–), 6.84 (d, $J = 8.3$ Hz, 2H, ArH), 6.70 (d, $J = 8.8$ Hz, 2H, ArH), 3.93 (t, $J = 6.2$ Hz, 2H, CH_2), 3.04 (s, 6H, $N(CH_3)_2$), 2.99–2.89 (m, 4H, CH_2), 2.38–2.21 (m, 8H, CH_2), 1.71 (s, 2H, CH_2), 1.36 (s, 11H, CH_2 and *tert*-Bu). ^{13}C NMR (101 MHz, $CDCl_3$) δ 188.84, 160.89, 155.01, 151.94, 145.01, 144.83, 143.73, 141.96, 130.24, 129.95, 129.64, 129.59, 127.91, 127.86, 126.70, 126.60, 123.63, 122.70, 121.11, 114.88, 111.90, 79.55, 77.38, 77.06, 76.74, 66.65, 53.40, 50.16, 47.21, 40.14, 30.05, 28.44, 27.22. HRMS (ESI): *m/z* calcd for $C_{71}H_{76}N_3O_4S_2$ 1098.5277; found 1098.5263 $[M + H]^+$.

4.7. tert-Butyl 2-((5-(4-((1E,4E)-5-(4-(dimethylamino)phenyl)-3-oxopenta-1,4-dienyl)phenoxy)pentyl)(2-(tritylthio)ethyl)amino)ethyl (2-(tritylthio)ethyl)carbamate (**4b**)

The procedure described above for the preparation of **4a** was employed to give **4b** (211.0 mg, 27.1%) as yellow solid foams. ^1H NMR (400 MHz, $CDCl_3$) δ 7.70 (d, $J = 15.8$ Hz, 1H, *trans* –CH=CH–), 7.68 (d, $J = 15.8$ Hz, 1H, *trans* –CH=CH–), 7.54 (d, $J = 7.7$ Hz, 2H, ArH), 7.52 (d, $J = 8.4$ Hz, 2H, ArH), 7.41–7.39 (m, 13H, ArH), 7.24–7.15 (m, 17H, ArH), 6.96 (d, $J = 15.8$ Hz, 1H, *trans* –CH = CH–), 6.89 (d, $J = 8.6$ Hz, 2H), 6.87 (d, $J = 15.9$ Hz, 1H, *trans* –CH = CH–), 6.69 (d, $J = 8.8$ Hz, 2H, ArH), 3.95 (t, $J = 6.4$ Hz, 2H, CH_2), 3.04 (s, 6H, $N(CH_3)_2$), 2.98–2.79 (m, 4H, CH_2), 2.39–2.17 (m, 10H, CH_2), 1.77–1.68 (m, 2H, CH_2), 1.36 (s, 13H, CH_2 and *tert*-Bu). ^{13}C NMR (101 MHz, $CDCl_3$) δ 188.81, 160.93, 155.01, 151.95, 145.04, 144.86, 143.73, 141.89, 130.23, 129.96, 129.67, 127.91, 127.85, 126.69, 126.61, 123.69, 122.72, 121.11, 114.89, 111.91, 79.47, 77.39, 77.07, 76.75, 68.04, 66.68, 53.38, 47.09, 40.13, 29.94, 29.07, 28.46, 27.12, 23.72. HRMS (ESI): *m/z* calcd for $C_{73}H_{80}N_3O_4S_2$ 1126.5590; found 1126.5538 $[M + H]^+$.

4.8. 2-((3-(4-((1E,4E)-5-(4-(Dimethylamino)phenyl)-3-oxopenta-1,4-dienyl)phenoxy)propyl)(2-(tritylthio)ethyl)amino)-N-(2-(tritylthio) ethyl)acetamide (**4c**)

A mixture of **3b** (414.3 mg, 1.0 mmol), *N*-(2-(tritylthio)ethyl)-2-(2-(tritylthio)ethylamino)acetamide (622.8 mg, 1.0 mmol) and K_2CO_3 (276.4 mg, 2.0 mmol) in acetonitrile (50 mL) was stirred at 90 °C for 48 h. The solvent was removed by vacuum, and water was added. The mixture was extracted with $CHCl_3$. The organic layers were combined and dried over Na_2SO_4 and evaporated dry. The crude product was purified by silica gel chromatography (petroleum ether/AcOEt = 3/1, v/v) to give **4c** (502.3 mg, 50.8%) as yellow solid foams. ^1H NMR (400 MHz, $CDCl_3$) δ 7.71 (d, $J = 15.8$ Hz, 1H, *trans* –CH=CH–), 7.66 (d, $J = 15.8$ Hz, 1H, *trans* –CH=CH–), 7.52 (d, $J = 8.8$ Hz, 2H, ArH), 7.45 (d, $J = 8.5$ Hz, 2H, ArH), 7.38–7.33 (m, 13H, ArH), 7.24–7.18 (m, 17H, ArH), 6.94 (d, $J = 15.8$ Hz, 1H, *trans* –CH=CH–), 6.88 (d, $J = 15.7$ Hz, 1H, *trans* –CH=CH–), 6.82 (d, $J = 8.7$ Hz, 2H, ArH), 6.69 (d, $J = 8.9$ Hz, 2H, ArH), 3.95 (t, $J = 5.9$ Hz, 2H, CH_2), 3.04 (s, 6H, $N(CH_3)_2$), 3.03–2.98 (m, 2H, CH_2), 2.90 (s, 2H, CH_2), 2.50 (t, $J = 6.9$ Hz, 2H, CH_2), 2.40 (t, $J = 6.5$ Hz, 2H, CH_2), 2.35 (t, $J = 6.3$ Hz, 2H, CH_2), 2.28 (t, $J = 6.5$ Hz, 2H, CH_2), 1.84–1.77 (m, 2H, CH_2). ^{13}C NMR (101 MHz, $CDCl_3$) δ 188.80, 170.96, 160.60, 151.96, 144.74, 143.81, 141.84, 130.26, 129.96, 129.56, 129.55, 127.94, 127.89, 126.74, 123.77, 122.66, 121.08, 114.85, 111.91, 77.41, 77.10, 76.78, 66.88, 66.78, 65.71, 58.47, 54.10, 51.19, 40.13, 38.06, 32.11, 30.09, 26.97. HRMS (ESI): *m/z* calcd for $C_{66}H_{66}N_3O_3S_2$ 1012.4546; found 1012.4502 $[M + H]^+$.

4.9. 2-((5-(4-((1E,4E)-5-(4-(Dimethylamino)phenyl)-3-oxopenta-1,4-dienyl)phenoxy)pentyl)(2-(tritylthio)ethyl)amino)-N-(2-(trityl thio)ethyl)acetamide (**4d**)

The procedure described above for the preparation of **4c** was employed to give **4d** (549.6 mg, 54.1%) as yellow solid foams. ^1H NMR (400 MHz, $CDCl_3$) δ 7.70 (d, $J = 15.7$ Hz, 1H, *trans* –CH=CH–), 7.67 (d, $J = 15.8$ Hz, 1H, *trans* –CH=CH–), 7.52 (d, $J = 8.7$ Hz, 2H, ArH), 7.52 (d, $J = 8.9$ Hz, 2H, ArH), 6.96 (d, $J = 15.8$ Hz, 1H, *trans* –CH=CH–), 6.87 (d, $J = 15.6$ Hz, 1H, *trans* –CH=CH–), 6.85 (d, $J = 8.6$ Hz, 2H, ArH), 6.69 (d, $J = 8.8$ Hz, 2H, ArH), 3.89 (t, $J = 6.3$ Hz,

2H, CH_2), 3.04 (s, 6H, $N(CH_3)_2$), 3.01 (m, 2H, CH_2), 2.85 (s, 2H, CH_2), 2.44–2.34 (m, 4H, CH_2), 2.33–2.22 (m, 4H, CH_2), 1.74–1.66 (m, 2H, CH_2), 1.38 (s, 4H, CH_2). ^{13}C NMR (101 MHz, $CDCl_3$) δ 188.82, 171.19, 160.82, 151.95, 144.77, 144.74, 143.79, 141.87, 130.25, 129.97, 129.56, 127.93, 127.77, 126.72, 123.71, 122.67, 121.07, 114.86, 111.90, 77.40, 77.08, 76.76, 67.86, 66.81, 66.74, 58.33, 54.72, 53.95, 40.14, 37.99, 32.07, 30.06, 29.01, 26.97, 23.79. HRMS (ESI): *m/z* calcd for $C_{68}H_{70}N_3O_3S_2$ 1040.4859; found 1040.4801 $[M + H]^+$.

4.10. (1E,4E)-1-(4-(Dimethylamino)phenyl)-5-(4-(3-((2-mercapto ethyl)(2-(2-mercaptoethylamino)ethyl)amino)propoxy)phenyl) penta-1,4-dien-3-one-rhenium (V) oxide (**5a**)

A solution of **4a** (157.8 mg, 0.15 mmol) in TFA (2 mL) was stirred at room temperature for 5 min. Triethylsilane (60 μL) was added and the mixture was stirred at 0 °C for 10 min, then the solvent was removed in vacuum. The residue was redissolved in a mixed solvent (10 mL, CH_2Cl_2/CH_3OH = 10/1, v/v), $(Ph_3P)_2ReOCl_3$ (122.3 mg, 0.15 mmol) and sodium acetate in methanol (1 M, 2 mL) were added. The reaction mixture was heated to reflux for 4 h. After cooling to room temperature, the solvent was evaporated. Then water was added and the resulting mixture was extracted by CH_2Cl_2 (3 × 15 mL), the combined organic layer was dried over anhydrous $MgSO_4$. After the solvent was removed, the residue was purified by silica gel chromatography (CH_2Cl_2/CH_3OH = 400/1, v/v) to give **5a** (28.9 mg, 27.6%) as an orange solid. m.p. 122.8–123.4 °C. ^1H NMR (400 MHz, $CDCl_3$) δ 7.71 (d, J = 15.3 Hz, 1H, *trans* −CH═CH−), 7.67 (d, J = 15.4 Hz, 1H, *trans* −CH═CH−), 7.57 (d, J = 8.6 Hz, 2H, ArH), 7.52 (d, J = 8.7 Hz, 2H, ArH), 6.98 (d, J = 15.8 Hz, 1H, *trans* −CH═CH−), 6.90 (d, J = 8.9 Hz, 2H, ArH), 6.87 (d, J = 16.6 Hz, 1H, *trans* −CH═CH−), 6.69 (d, J = 8.7 Hz, 2H, ArH), 4.32–4.21 (m, 1H, CH_2), 4.16 (dd, J = 10.4, 6.2 Hz, 2H, CH_2), 4.10 (s, 2H, CH_2), 3.97–3.86 (m, 1H, CH_2), 3.85–3.74 (m, 2H, CH_2), 3.45–3.35 (m, 2H, CH_2), 3.32–3.24 (m, 1H, CH_2), 3.04 (s, 6H, $N(CH_3)_2$), 2.83–2.74 (m, 1H, CH_2), 2.35–2.31 (m, 2H, CH_2), 1.79 (td, J = 11.9, 4.6 Hz, 2H, CH_2), 0.90–0.78 (m, 2H, CH_2). ^{13}C NMR (101 MHz, $CDCl_3$) δ 188.79, 159.79, 151.98, 143.93, 141.43, 130.29, 130.02, 128.57, 124.18, 122.66, 121.03, 114.80, 111.92, 77.31, 77.00, 76.68, 70.89, 65.48, 64.95, 62.67, 60.62, 59.14, 49.40, 40.11, 29.65, 23.41. HRMS (ESI): *m/z* calcd for $C_{28}H_{37}N_3O_3ReS_2$ 714.1834; found 714.2107 $[M + H]^+$.

4.11. (1E,4E)-1-(4-(Dimethylamino)phenyl)-5-(4-(5-((2-mercapto ethyl)(2-(2-mercaptoethylamino)ethyl)amino)pentyloxy)phenyl) penta-1,4-dien-3-one-rhenium (V) oxide (**5b**)

The procedure described above for the preparation of **5a** was employed to give **5b** (30.1 mg, 29.6%) as an orange solid. m.p. 154.5–155.3 °C. ^1H NMR (400 MHz, $CDCl_3$) δ 7.70 (d, J = 15.7 Hz, 1H, *trans* −CH═CH−), 7.67 (d, J = 15.8 Hz, 1H, *trans* −CH═CH−), 7.56 (d, J = 8.6 Hz, 2H, ArH), 7.51 (d, J = 8.8 Hz, 2H, ArH), 6.97 (d, J = 15.8 Hz, 1H, *trans* −CH═CH−), 6.90 (d, J = 8.7 Hz, 2H, ArH), 6.87 (d, J = 15.8 Hz, 1H, *trans* −CH═CH−), 6.69 (d, J = 8.8 Hz, 2H, ArH), 4.18–4.09 (m, 2H, CH_2), 4.02 (t, J = 6.1 Hz, 2H, CH_2), 3.89–3.82 (m, 1H, CH_2), 3.77 (dd, J = 11.2, 5.2 Hz, 1H, CH_2), 3.61–3.51 (m, 1H, CH_2), 3.41–3.31 (m, 3H, CH_2), 3.29–3.18 (m, 1H, CH_2), 3.04 (s, 6H, $N(CH_3)_2$), 3.00–2.93 (m, 2H, CH_2), 2.73 (dd, J = 13.4, 3.1 Hz, 1H, CH_2), 1.92–1.82 (m, 4H, CH_2), 1.76–1.65 (m, 2H, CH_2), 1.63–1.51 (m, 2H, CH_2). ^{13}C NMR (101 MHz, $CDCl_3$) δ 188.78, 160.58, 151.96, 143.85, 141.67, 130.24, 129.97, 128.02, 123.86, 122.64, 121.01, 114.84, 111.89, 77.33, 77.01, 76.69, 70.92, 67.53, 65.48, 63.60, 62.75, 58.89, 49.14, 40.12, 40.00, 28.83, 23.76, 22.83. HRMS (ESI): *m/z* calcd for $C_{30}H_{41}N_3O_3ReS_2$ 742.2147; found 742.2329 $[M + H]^+$.

4.12. 2-((3-(4-((1E,4E)-5-(4-(Dimethylamino)phenyl)-3-oxopenta-1,4-dienyl)phenoxy)propyl)(2-mercaptoethyl)amino)-N-(2-mercapto ethyl)acetamide-rhenium (V) oxide (**5c**)

The procedure described above for the preparation of **5a** was employed to give **5c** (57.4 mg, 15.5%) as an orange solid. m.p. 116.3–117.5 °C. ^1H NMR (400 MHz, $CDCl_3$) δ 7.71 (d, J = 16.2 Hz, 1H, *trans* −CH═CH−), 7.67 (d, J = 16.6 Hz, 1H, *trans* −CH═CH−), 7.57 (d, J = 8.7 Hz, 2H, ArH), 7.52 (d, J = 8.8 Hz, 2H, ArH), 6.98 (d, J = 15.8 Hz, 1H, *trans* −CH═CH−), 6.91 (d, J = 8.7 Hz, 2H, ArH), 6.87 (d, J = 15.8 Hz, 1H, *trans* −CH═CH−), 6.70 (d, J = 8.7 Hz, 2H, ArH), 4.73 (d, J = 16.4 Hz, 1H, CH_2), 4.60 (dd, J = 11.7, 5.5 Hz, 1H, CH_2), 4.15 (d, J = 16.9 Hz, 2H, CH_2), 4.12–4.07 (m, 2H, CH_2), 3.85–3.75 (m, 1H, CH_2), 3.48–3.40 (m, 1H, CH_2), 3.32–3.24 (m, 2H, CH_2), 3.23–3.19 (m, 1H, CH_2), 3.05 (s, 6H, $N(CH_3)_2$), 2.93–2.89 (m, 1H, CH_2), 2.50–2.41 (m, 1H, CH_2), 2.37–2.24 (m, 3H, CH_2). ^{13}C NMR (101 MHz, $CDCl_3$) δ 188.67, 186.86, 159.57, 155.59, 151.94, 143.95, 141.30, 130.24, 129.99, 128.53, 125.00, 124.30, 121.00, 114.77, 111.92, 77.31, 76.99, 76.68, 66.83, 64.54, 60.77, 59.88, 48.07, 40.15, 39.03, 32.20, 29.67, 26.40, 24.13, 23.41. HRMS (ESI): *m/z* calcd for $C_{28}H_{35}N_3O_4ReS_2$ 728.1626; found 728.1600 $[M + H]^+$.

4.13. 2-((5-(4-((1E,4E)-5-(4-(Dimethylamino)phenyl)-3-oxopenta-1,4-dienyl)phenoxy)pentyl)(2-mercaptoethyl)amino)-N-(2-mercapto ethyl)acetamide-rhenium (V) oxide (**5d**)

The procedure described above for the preparation of **5a** was employed to give **5d** (56.0 mg, 37.0%) as an orange solid. m.p. 121.7–122.3 °C. ^1H NMR (400 MHz, $CDCl_3$) δ 7.70 (d, J = 15.6 Hz, 1H, *trans* −CH═CH−), 7.67 (d, J = 15.7 Hz, 1H, *trans* −CH═CH−), 7.56 (d, J = 8.5 Hz, 2H, ArH), 7.52 (d, J = 8.7 Hz, 2H, ArH), 6.98 (d, J = 15.9 Hz, 1H, *trans* −CH═CH−), 6.90 (d, J = 8.8 Hz, 2H, ArH), 6.87 (d, J = 15.8 Hz, 1H, *trans* −CH═CH−), 6.69 (d, J = 8.6 Hz, 2H, ArH), 4.66 (d, J = 16.4 Hz, 1H, CH_2), 4.58 (dd, J = 11.5, 5.3 Hz, 1H, CH_2), 4.12 (d, J = 16.2 Hz, 1H, CH_2), 4.08–3.93 (m, 3H, CH_2), 3.59–3.52 (m, 1H, CH_2), 3.41–3.33 (m, 1H, CH_2), 3.27–3.17 (m, 3H, CH_2), 3.04 (s, 6H, $N(CH_3)_2$), 2.87 (dd, J = 13.5, 4.1 Hz, 1H, CH_2), 1.93–1.85 (m, 4H, CH_2), 1.68–1.56 (m, 4H, CH_2). ^{13}C NMR (101 MHz, $CDCl_3$) δ 188.77, 186.94, 160.45, 151.94, 143.85, 141.61, 130.23, 129.98, 128.17, 123.94, 122.73, 121.06, 114.80, 111.93, 77.30, 76.98, 76.67, 67.40, 67.00, 64.21, 63.68, 59.83, 47.91, 40.14, 38.95, 29.67, 28.71, 23.73, 23.55. HRMS (ESI): *m/z* calcd for $C_{30}H_{39}N_3O_4ReS_2$ 756.1939; found 756.1945 $[M + H]^+$.

4.14. In vitro fluorescent staining using Tg mouse brain sections

The transgenic model mice (C57BL6, APPswe/PSEN1, 11 months old) and age-matched control mice (C57BL6, 11 months old) were used for the studies. Paraffin-embedded brain sections (10 μm thick) were deparaffinized with 3 × 10 min washes in xylene, 2 × 5 min washes in 100% ethanol, 5 min wash in 80% ethanol/H_2O, 5 min wash in 60% ethanol/H_2O, and 10 min wash in running tap water and then incubated in PBS (0.2 M, pH = 7.4) for 30 min. The brain sections were incubated with a 10% ethanol solution (1.0 μM) of **5a**, **5b**, **5c** and **5d** for 10 min, respectively. The locations of plaques were confirmed by staining with Thioflavin-S (0.125%) in adjacent sections. Finally, the sections were washed with 40% ethanol for 10 min. Fluorescent observation was performed by the Axio Observer Z1 inverted fluorescence microscope (Zeiss, Germany) equipped with DAPI (excitation, 405 nm) and AF (excitation, 495 nm) filter sets.

4.15. Binding assay in vitro using Aβ aggregates

Peptides $A\beta_{(1-42)}$ were purchased from Osaka Peptide Institute (Osaka, Japan). Aggregation was carried out by gently dissolving the

peptide [0.56 mg/mL for A$\beta_{(1-42)}$] in a buffer solution (pH = 7.4) containing 10 mM sodium phosphate and 1 mM EDTA. The solution was incubated at 37 °C for 42 h with gentle and constant shaking. Inhibition experiments were carried out in 12 × 75 mm borosilicate glass tubes according to procedures described previously with some modification. Briefly, 100 μL of A$\beta_{(1-42)}$ aggregates (28 nM in the final assay mixture) was added into a mixture containing 100 μL of radioligand ([^{125}I]IMPY, 100,000 cpm/100 μL), 100 μL of inhibitors (**5a**, **5b**, **5c** or **5d**, 10^{-4} to $10^{-8.5}$ M in ethanol), and 700 μL of PBS (0.2 M, pH = 7.4) containing 0.5% BSA in a final volume of 1 mL. Non-specific binding was defined in the presence of 1 μM IMPY. The mixture was incubated at room-temperature for 3 h, and then the bound and free radioactive fractions were separated by vacuum filtration through borosilicate glass fiberfilters (Whatman GF/B) using an Mp-48T cell harvester (Brandel, Gaithersburg, MD). The radioactivity of filters containing the bound ^{125}I-ligand was measured in an automatic γ-counter (WALLAC/Wizard1470, USA) with 70% efficiency. Under the assay conditions, the specifically bound fraction accounted for about 10% of total radioactivity. The half-maximal inhibitory concentration (IC_{50}) was determined from displacement curves of three independent experiments using GraphPad Prism 5.0, and the inhibition constant (K_i) was calculated using the Cheng-Prusoff inhibition constant equation: $K_i = IC_{50}/(1 + [L]/K_d)$, where [$L$] represents the concentration of [^{125}I]IMPY used in the assay and K_d is the dissociation constant of [^{125}I]IMPY.

4.16. ^{99m}Tc labeling reaction and analysis by HPLC

Na^{99m}TcO$_4$ solution (74 MBq, 200 μL) was added to a GH kit and reacted at room temperature for 10 min to give a ^{99m}Tc-GH solution. To a solution of precursor (**4a**–**d**, 0.5 mg) in TFA (200 μL) was added triethylsilane (2 μL), and the mixture was left at room temperature for 10 min, then the solvents were removed under a stream of nitrogen gas. The residue was redissolved in ethanol (200 μL), and then mixed with the ^{99m}Tc-GH solution (200 μL). The reaction mixture was heated to 100 °C for 10 min. After cooling to room temperature, the product was extracted with $CHCl_3$ (2 × 1 mL) and then the solvents were removed under a stream of nitrogen gas. The residue was redissolved in 100 μL acetonitrile and purified by HPLC on a Venusil MP C18 reverse phase column (5 μm, 4.6 × 250 mm) with a binary gradient system (acetonitrile/water:70%/30%) at 1.0 mL/min flow rate to give [^{99m}Tc]**5a**, [^{99m}Tc]**5b**, [^{99m}Tc]**5c** and [^{99m}Tc]**5d**, respectively. The identity of [^{99m}Tc]**5a**–**d** was verified by a comparison of the retention time with that of the nonradioactive rhenium complexes from the HPLC profiles. The four ^{99m}Tc-complexes were proven to show >95% radiochemical purity by HPLC.

4.17. Partition coefficient determination

The log D values of [^{99m}Tc]**5a**, [^{99m}Tc]**5b**, [^{99m}Tc]**5c** and [^{99m}Tc]**5d** were determined by measuring the distribution of the radiotracer between 1-octanol and PBS buffer at pH = 7.4. The two phases were pre-saturated with each other. 1-Octanol (3.6 mL) and PBS (3.0 mL) were pipetted into a 10 mL plastic centrifuge tube containing 740 kBq of ^{99m}Tc-labeled tracers. The mixture was vortexed for 5 min, followed by centrifugation for 5 min (3500 rpm, Anke TDL80-2B, China). 50 μL of the 1-octanol layer and 500 μL of the buffer layer were deposed in two test tubes for counting. The amount of radioactivity in each tube was measured with an automatic γ-counter (Wallac 1470 Wizard, USA). The measurement was carried out in triplicate and repeated three times. The distribution coefficient was determined by calculating the ratio of cpm/mL of 1-octanol phase versus that of PBS phase and expressed as log D. Then 2.0 mL of the remaining 1-octanol layer was transferred into a new centrifuge tube, and new 1-octanol (1.6 mL) and PBS (3.0 mL) were pipetted into it. The vortexing, centrifuging, and counting protocols were repeated until consistent distribution coefficient values were obtained.

4.18. Biodistribution in normal mice

A saline solution containing the HPLC-purified ^{99m}Tc-labled tracer (100 μL, 10% ethanol, 185 kBq) was injected intravenously into ICR mice (five weeks, male) via the tail vein. The mice ($n = 5$ for each time point) were sacrificed by decapitation exactly at 2, 10, 30, and 60 min post-injection. Samples of blood and organs of interest were removed, weighed and radioactivity was counted with an automatic γ-counter (Wallac 1470 Wizard, USA). The results were expressed in terms of the percentage of the injected dose per gram (%ID/g) of blood or organs.

Acknowledgments

The authors present special thanks to Dr. Jin Liu (College of Life Science, Beijing Normal University) for assistance in the *in vitro* neuropathological staining. This work was funded by National Natural Science Foundation of China (No: 21201019), Research Fund for the Doctoral Program of Higher Education of China (No: 20120003120013) and Fundamental Research Funds for the Central Universities (No: 2012LYB19).

Appendix A. Supplementary data

Supplementary data related to this article can be found at http://dx.doi.org/10.1016/j.ejmech.2013.03.057.

References

[1] D.J. Selkoe, The origins of Alzheimer disease: A is for amyloid, JAMA 283 (2000) 1615–1617.
[2] D.J. Selkoe, Alzheimer's disease: genes, proteins, and therapy, Physiol. Rev. 81 (2001) 741–766.
[3] A. Wimo, B. Winblad, H. Aguero-Torres, E. von Strauss, The magnitude of dementia occurrence in the world, Alzheimer Dis. Assoc. Disord. 17 (2003) 63–67.
[4] J. Hardy, D.J. Selkoe, The amyloid hypothesis of Alzheimer's disease: progress and problems on the road to therapeutics, Science 297 (2002) 353–356.
[5] J.L. Cummings, Alzheimer's disease, N. Engl. J. Med. 351 (2004) 56–67.
[6] B.C.P. Lee, M. Mintun, R.L. Buckner, J.C. Morris, Imaging of Alzheimer's disease, J. Neuroimaging 13 (2003) 199–214.
[7] V.L. Villemagne, C.C. Rowe, S. Macfarlane, K.E. Novakovic, C.L. Masters, Imaginem oblivionis: the prospects of neuroimaging for early detection of Alzheimer's disease, J. Clin. Neurosci. 12 (2005) 221–230.
[8] H. Braak, E. Braak, Neuropathological stageing of Alzheimer-related changes, Acta Neuropathol. 82 (1991) 239–259.
[9] M. Ono, A. Wilson, J. Nobrega, D. Westaway, P. Verhoeff, Z.-P. Zhuang, M.-P. Kung, H.F. Kung, ^{11}C-labeled stilbene derivatives as Aβ-aggregate-specific PET imaging agents for Alzheimer's disease, Nucl. Med. Biol. 30 (2003) 565–571.
[10] N.P.L.G. Verhoeff, A.A. Wilson, S. Takeshita, L. Trop, D. Hussey, K. Singh, H.F. Kung, M.-P. Kung, S. Houle, In-vivo imaging of Alzheimer disease [beta]-amyloid with [^{11}C]SB-13 PET, Am. J. Geriatr. Psychiatry 12 (2004) 584–595.
[11] W.E. Klunk, H. Engler, A. Nordberg, Y. Wang, G. Blomqvist, D.P. Holt, M. Bergström, I. Savitcheva, G.-F. Huang, S. Estrada, B. Ausén, M.L. Debnath, J. Barletta, J.C. Price, J. Sandell, B.J. Lopresti, A. Wall, P. Koivisto, G. Antoni, C.A. Mathis, B. Långström, Imaging brain amyloid in Alzheimer's disease with Pittsburgh compound-B, Ann. Neurol. 55 (2004) 306–319.
[12] C.A. Mathis, Y. Wang, D.P. Holt, G.-F. Huang, M.L. Debnath, W.E. Klunk, Synthesis and evaluation of ^{11}C-labeled 6-substituted 2-arylbenzothiazoles as amyloid imaging agents, J. Med. Chem. 46 (2003) 2740–2754.
[13] C.C. Rowe, U. Ackerman, W. Browne, R. Mulligan, K.L. Pike, G. O'Keefe, H. Tochon-Danguy, G. Chan, S.U. Berlangieri, G. Jones, K.L. Dickinson-Rowe, H.P. Kung, W. Zhang, M.P. Kung, D. Skovronsky, T. Dyrks, G. Holl, S. Krause, M. Friebe, L. Lehman, S. Lindemann, L.M. Dinkelborg, C.L. Masters, V.L. Villemagne, Imaging of amyloid β in Alzheimer's disease with ^{18}F-BAY94-9172, a novel PET tracer: proof of mechanism, Lancet Neurol. 7 (2008) 129–135.
[14] V.L. Villemagne, K. Ong, R.S. Mulligan, G. Holl, S. Pejoska, G. Jones, G. O'Keefe, U. Ackerman, H. Tochon-Danguy, J.G. Chan, C.B. Reininger, L. Fels, B. Putz,

B. Rohde, C.L. Masters, C.C. Rowe, Amyloid imaging with ^{18}F-florbetaben in Alzheimer disease and other dementias, J. Nucl. Med. 52 (2011) 1210–1217.
[15] M.T. Fodero-Tavoletti, D. Brockschnieder, V.L. Villemagne, L. Martin, A.R. Connor, A. Thiele, M. Berndt, C.A. McLean, S. Krause, C.C. Rowe, C.L. Masters, L. Dinkelborg, T. Dyrks, R. Cappai, In vitro characterization of [^{18}F]-florbetaben, an Aβ imaging radiotracer, Nucl. Med. Biol. 39 (2012) 1042–1048.
[16] M. Koole, D.M. Lewis, C. Buckley, N. Nelissen, M. Vandenbulcke, D.J. Brooks, R. Vandenberghe, K. Van Laere, Whole-body biodistribution and radiation dosimetry of ^{18}F-GE067: a radioligand for in vivo brain amyloid imaging, J. Nucl. Med. 50 (2009) 818–822.
[17] K.J. Lin, W.C. Hsu, I.T. Hsiao, S.P. Wey, L.W. Jin, D. Skovronsky, Y.Y. Wai, H.P. Chang, C.W. Lo, C.H. Yao, T.C. Yen, M.P. Kung, Whole-body biodistribution and brain PET imaging with [^{18}F]AV-45, a novel amyloid imaging agent-a pilot study, Nucl. Med. Biol. 37 (2010) 497–508.
[18] S.R. Choi, G. Golding, Z. Zhuang, W. Zhang, N. Lim, F. Hefti, T.E. Benedum, M.R. Kilbourn, D. Skovronsky, H.F. Kung, Preclinical properties of ^{18}F-AV-45: a PET agent for Aβ plaques in the brain, J. Nucl. Med. 50 (2009) 1887–1894.
[19] D.F. Wong, P.B. Rosenberg, Y. Zhou, A. Kumar, V. Raymont, H.T. Ravert, R.F. Dannals, A. Nandi, J.R. Brašić, W. Ye, J. Hilton, C. Lyketsos, H.F. Kung, A.D. Joshi, D.M. Skovronsky, M.J. Pontecorvo, Vivo imaging of amyloid deposition in Alzheimer disease using the radioligand ^{18}F-AV-45 (Florbetapir F 18), J. Nucl. Med. 51 (2010) 913–920.
[20] H. Han, C.-G. Cho, P.T. Lansbury, Technetium complexes for the quantitation of brain amyloid, J. Am. Chem. Soc. 118 (1996) 4506–4507.
[21] W. Zhen, H. Han, M. Anguiano, C.A. Lemere, C.G. Cho, P.T. Lansbury, Synthesis and amyloid binding properties of rhenium complexes: preliminary progress toward a reagent for SPECT imaging of Alzheimer's disease brain, J. Med. Chem. 42 (1999) 2805–2815.
[22] N.A. Dezutter, R.J. Dom, T.J. de Groot, G.M. Bormans, A.M. Verbruggen, ^{99m}Tc-MAMA-chrysamine G, a probe for beta-amyloid protein of Alzheimer's disease, Eur. J. Nucl. Med. 26 (1999) 1392–1399.
[23] N.A. Dezutter, T.J. de Groot, R.H. Busson, G.A. Janssen, A.M. Verbruggen, Preparation of ^{99m}Tc-N_2S_2 conjugates of chrysamine G, potential probes for the beta-amyloid protein of Alzheimer's disease, J. Labelled Comp. Radiopharm. 42 (1999) 309–324.
[24] Z.-P. Zhuang, M.-P. Kung, C. Hou, K. Ploessl, H.F. Kung, Biphenyls labeled with technetium 99m for imaging β-amyloid plaques in the brain, Nucl. Med. Biol. 32 (2005) 171–184.
[25] K. Serdons, T. Verduyckt, J. Cleynhens, C. Terwinghe, L. Mortelmans, G. Bormans, A. Verbruggen, Synthesis and evaluation of a ^{99m}Tc-BAT-phenylbenzothiazole conjugate as a potential in vivo tracer for visualization of amyloid β, Bioorg. Med. Chem. Lett. 17 (2007) 6086–6090.
[26] X. Chen, P. Yu, L. Zhang, B. Liu, Synthesis and biological evaluation of ^{99m}Tc, Re-monoamine-monoamide conjugated to 2-(4-aminophenyl)benzothiazole as potential probes for β-amyloid plaques in the brain, Bioorg. Med. Chem. Lett. 18 (2008) 1442–1445.
[27] K. Serdons, T. Verduyckt, J. Cleynhens, G. Bormans, A. Verbruggen, Development of ^{99m}Tc-thioflavin-T derivatives for detection of systemic amyloidosis, J. Labelled Comp. Radiopharm. 51 (2008) 357–367.
[28] M. Ono, R. Ikeoka, H. Watanabe, H. Kimura, T. Fuchigami, M. Haratake, H. Saji, M. Nakayama, Synthesis and evaluation of novel chalcone derivatives with ^{99m}Tc/Re complexes as potential probes for detection of β-amyloid plaques, ACS Chem. Neurosci. 1 (2010) 598–607.
[29] M. Ono, R. Ikeoka, H. Watanabe, H. Kimura, T. Fuchigami, M. Haratake, H. Saji, M. Nakayama, ^{99m}Tc/Re complexes based on flavone and aurone as SPECT probes for imaging cerebral β-amyloid plaques, Bioorg. Med. Chem. Lett. 20 (2010) 5743–5748.
[30] M. Sagnou, D. Benaki, C. Triantis, T. Tsotakos, V. Psycharis, C.P. Raptopoulou, I. Pirmettis, M. Papadopoulos, M. Pelecanou, Curcumin as the OO bidentate ligand in "2 + 1" complexes with the $[M(CO)_3]^+$ (M = Re, ^{99m}Tc) tricarbonyl core for radiodiagnostic applications, Inorg. Chem. 50 (2011) 1295–1303.
[31] M. Ono, Y. Fuchi, T. Fuchigami, N. Kobashi, H. Kimura, M. Haratake, H. Saji, M. Nakayama, Novel benzofurans with ^{99m}Tc complexes as probes for imaging cerebral β-amyloid plaques, ACS Med. Chem. Lett. 1 (2010) 443–447.
[32] Y. Cheng, M. Ono, H. Kimura, M. Ueda, H. Saji, Technetium-99m labeled pyridyl benzofuran derivatives as single photon emission computed tomography imaging probes for β-amyloid plaques in Alzheimer's brains, J. Med. Chem. 55 (2012) 2279–2286.
[33] X. Wang, M. Cui, P. Yu, Z. Li, Y. Yang, H. Jia, B. Liu, Synthesis and biological evaluation of novel technetium-99m labeled phenylbenzoxazole derivatives as potential imaging probes for β-amyloid plaques in brain, Bioorg. Med. Chem. Lett. 22 (2012) 4327–4331.
[34] M. Cui, M. Ono, H. Kimura, B. Liu, H. Saji, Synthesis and structure–affinity relationships of novel dibenzylideneacetone derivatives as probes for β-amyloid plaques, J. Med. Chem. 54 (2011) 2225–2240.
[35] S.S. Jurisson, J.D. Lydon, Potential technetium small molecule radiopharmaceuticals, Chem. Rev. 99 (1999) 2205–2218.
[36] G. Tamagnan, R.M. Baldwin, N.S. Kula, R.J. Baldessarini, R.B. Innis, Cyclopentadienyltricarbonylrheniumbenzazepines: synthesis and binding affinity, Bioorg. Med. Chem. Lett. 10 (2000) 1113–1115.